Chapter 8

Perturbation Method for Solar/Infrared Radiative Transfer in a Scattering Medium with Vertical Inhomogeneity in Internal Optical Properties

Yi-Ning Shi, Feng Zhang, Jia-Ren Yan,
Qiu-Run Yu and Jiangnan Li

Additional information is available at the end of the chapter

http://dx.doi.org/10.5772/intechopen.77147

Abstract

A new scheme based on perturbation method is presented to solve the problem of solar/infrared radiative transfer (SRT/IRT) in a scattering medium, in which the inherent optical properties (IOPs) are vertically inhomogeneous. The Eddington approximation for SRT and the two-stream approximation for IRT are used as the zeroth-order solution, and multiple-scattering effect of inhomogeneous IOPs is included in the first-order solution. Observations show that the stratocumulus clouds are vertically inhomogeneous, and the accuracy of SRT/IRT for stratocumulus clouds by different solutions is evaluated. In the spectral band of 0.25–0.69 μm, the relative error in absorption with inhomogeneous SRT solution is 1.4% at most, but with the homogeneous SRT solution, it can be up to 7.4%. In the spectral band of 5–8 μm, the maximum relative error of downward emissivity can reach −11% for the homogeneous IRT solution but only −2% for the inhomogeneous IRT solution.

Keywords: perturbation method, radiative transfer, vertical inhomogeneity

1. Introduction

Solving the radiative transfer equation (RTE) is a key issue in radiation scheme for climate model and remote sensing. In most numerical radiative transfer algorithms, the atmosphere is divided into many homogeneous layers. The inherent optical properties (IOPs) are then fixed within each layer and the variations of IOPs inside each layer are ignored, effectively regarding each layer as internally homogeneous. The standard solar/infrared radiative transfer (SRT/IRT)

solutions are based on this assumption of internal homogeneity [1–4], which cannot resolve within-layer vertical inhomogeneity.

It has been well established by observation that cumulus and stratocumulus clouds (hereinafter, collectively referred to as cumulus clouds) are inhomogeneous, both horizontally and vertically [5–9]. Inside a cumulus cloud, the liquid water content (LWC) and the cloud droplet size distribution vary with height, and so the IOPs of cloud droplets depend on vertical height.

How to deal with vertical internal inhomogeneity in SRT/IRT models is an interesting topic for researchers. Li developed a Monte Carlo cloud model that can be used to investigate photon transport in inhomogeneous clouds by considering an internal variation of the optical properties [10]. Their model showed that when overcast clouds become broken clouds, the difference in reflectance at large solar zenith angles between vertically inhomogeneous clouds and their plane-parallel counterparts can be as much as 10%.

However, the Monte Carlo method is very expensive in computing and not applicable to climate models or remote sensing [11]. The albedo of inhomogeneous mixed-phase clouds at visible wavelengths could be obtained by using a Monte Carlo method to compare such clouds with plane-parallel homogeneous clouds [12].

In principle, the vertical inhomogeneity problem of the SRT/IRT process can be solved by increasing the number of layers of the climate model. However, it is time-consuming to increase the vertical resolution of a climate model. Typically, there are only 30–100 layers in a climate model [13], which is not high enough to resolve the cloud vertical inhomogeneity. To completely address the problem of vertical inhomogeneity by using a limited number of layers in a climate model, the standard SRT method must be extended to deal with the vertical inhomogeneity inside each model layer. The primary purpose of this study is to introduce a new inhomogeneous SRT/IRT solution presented by Zhang and Shi. This solution follows a perturbation method: the zeroth-order solution is the standard Eddington approximation for SRT and two-stream approximation for IRT, with a first-order perturbation to account for the inhomogeneity effect. In Section 2, the basic theory of SRT/IRT is introduced, and the new inhomogeneous SRT/IRT solution is presented. In Section 3, the inhomogeneous SRT/IRT solution is applied to cloud as realistic examples to demonstrate the practicality of this new method. A summary is given in Section 4.

2. SRT/IRT solution for an inhomogeneous layer

2.1. SRT solution

The azimuthally averaged solar radiative transfer equation [1–4, 10–12] is

$$\mu \frac{dI_S(\tau,\mu)}{d\tau} = I_S(\tau,\mu) - \frac{\omega(\tau)}{2}\int_{-1}^{1} I_S(\tau,\mu)P(\tau,\mu,\mu')d\mu' - \frac{\omega(\tau)}{4\pi}F_0 P(\tau,\mu,-\mu_0)e^{-\frac{\tau}{\mu_0}} \tag{1}$$

where μ is the cosine of the zenith angle ($\mu > 0$ and $\mu < 0$ refer to upward and downward radiation, respectively), $P(\tau,\mu,\mu')$ is the scattering phase function, τ is the optical depth

($\tau = 0$ and $\tau = \tau_0$ refer to the top and bottom of the medium, respectively), $\omega(\tau)$ is the single-scattering albedo, and F_0 is the incoming solar flux. For the Eddington approximation, $P(\tau, \mu, \mu') = 1 + 3g(\tau)\mu\mu'$ ($-1 < \mu < 1$) and $g(\tau)$ are the asymmetry factors. For the scattering atmosphere, the irradiance fluxes in the upward and downward directions can be written as

$$F_S^{\pm}(\tau) = 2\pi \int_0^{\pm 1} I_S(\tau, \mu)\mu d\mu \tag{2}$$

To simulate a realistic medium such as cloud or snow, we consider $\omega(\tau)$ and $g(\tau)$ to vary with τ, and we use exponential expressions here to simplify the process. The single-scattering albedo and asymmetry factor are written as

$$\omega(\tau) = \widehat{\omega} + \varepsilon_\omega \left(e^{-a_1 \tau} - e^{-a_1 \tau_0/2} \right) \tag{3a}$$

$$g(\tau) = \widehat{g} + \varepsilon_g \left(e^{-a_2 \tau} - e^{-a_2 \tau_0/2} \right) \tag{3b}$$

where τ_0 is the optical depth of the layer, $\widehat{\omega}$ is the single-scattering albedo at $\tau_0/2$, and $\widehat{g}$ is the asymmetry factor at the same place. Both ε_g and ε_ω are small parameters that are far less than $\widehat{g}$ and $\widehat{\omega}$, respectively, in a realistic medium.

According to the Eddington approximation, the radiative intensity $I_S(\tau, \mu)$ can be written as

$$I_S(\tau, \mu) = I_{S0}(\tau) + I_{S1}(\tau)\mu \tag{4}$$

Using Eqs. (1), (2), and (4), we obtain

$$\frac{dF_S^+(\tau)}{d\tau} = \gamma_1(\tau)F_S^+(\tau) - \gamma_2(\tau)F_S^-(\tau) - \gamma_3(\tau)\omega(\tau)F_0 e^{-\frac{\tau}{\mu_0}} \tag{5a}$$

$$\frac{dF_S^-(\tau)}{d\tau} = \gamma_2(\tau)F_S^+(\tau) - \gamma_1(\tau)F_S^-(\tau) + \left[1 - \gamma_3(\tau)\right]\omega(\tau)F_0 e^{-\frac{\tau}{\mu_0}} \tag{5b}$$

$$F_S^-(0) = 0, F_S^+(\tau_0) = R_{dif}F_S^-(\tau_0) + R_{dir}\mu_0 F_0 e^{-\frac{\tau_0}{\mu_0}} \tag{5c}$$

where $\gamma_1(\tau) = \frac{1}{4}\{7 - [4 + 3g(\tau)]\omega(\tau)\}$, $\gamma_2(\tau) = \frac{-1}{4}\{1 - [4 - 3g(\tau)]\omega(\tau)\}$, and $\gamma_3(\tau) = \frac{1}{4}\left[2 - 3g(\tau)\mu_0\right]$; τ_0 is the optical depth of the single layer; and R_{dif}(R_{dir}) is the diffuse (resp., direct) reflection from the layer below or the diffuse (direct) surface albedo. Substituting $\gamma_1(\tau)$, $\gamma_2(\tau)$, and $\gamma_3(\tau)$ into Eq. (3) and ignoring the small second-order parameters ${\varepsilon_\omega}^2$, ${\varepsilon_g}^2$, and $\varepsilon_\omega\varepsilon_g$, we get

$$\gamma_1(\tau) = \gamma_1^0 + \gamma_1^1\varepsilon_\omega \left(e^{-a_1 \tau} - e^{-a_1 \tau_0/2} \right) + \gamma_1^2\varepsilon_g \left(e^{-a_2 \tau} - e^{-a_2 \tau_0/2} \right) \tag{6a}$$

$$\gamma_2(\tau) = \gamma_2^0 + \gamma_2^1\varepsilon_\omega \left(e^{-a_1 \tau} - e^{-a_1 \tau_0/2} \right) + \gamma_2^2\varepsilon_g \left(e^{-a_2 \tau} - e^{-a_2 \tau_0/2} \right) \tag{6b}$$

$$\gamma_3(\tau) = \gamma_3^0 + \gamma_3^2\varepsilon_g \left(e^{-a_2 \tau} - e^{-a_2 \tau_0/2} \right) \tag{6c}$$

where $\gamma_1^0 = \frac{1}{4}[7-(4+3\widehat{g})\widehat{\omega}]$, $\gamma_2^0 = \frac{-1}{4}[1-(4-3\widehat{g})\widehat{\omega}]$, $\gamma_3^0 = \frac{1}{4}(2-3\widehat{g}\mu_0)$, $\gamma_1^1 = \frac{-1}{4}(4+3\widehat{g})$, $\gamma_1^2 = -\frac{3}{4}\widehat{\omega}$, $\gamma_2^1 = \frac{1}{4}(4-3\widehat{g})$, $\gamma_2^2 = -\frac{3}{4}\widehat{\omega}$, and $\gamma_3^2 = -\frac{3}{4}\mu_0$.

By perturbation theory [14], the corresponding flux can also be expanded by using the perturbation coefficients ε_ω and ε_g:

$$F_S^+ = F_{S0}^+ + \varepsilon_\omega F_{S1}^+ + \varepsilon_g F_{S2}^+ \tag{7a}$$

$$F_S^- = F_{S0}^- + \varepsilon_\omega F_{S1}^- + \varepsilon_g F_{S2}^- \tag{7b}$$

Substituting Eqs. (6) and (7) into Eq. (5) yields

$$\begin{aligned}\frac{dF_S^+}{d\tau} = &\left[\gamma_1^0 + \gamma_1^1\varepsilon_\omega\left(e^{-a_1\tau} - e^{-a_1\tau_0/2}\right) + \gamma_1^2\varepsilon_g\left(e^{-a_2\tau} - e^{-a_2\tau_0/2}\right)\right]\left(F_{S0}^+ + \varepsilon_\omega F_{S1}^+ + \varepsilon_g F_{S2}^+\right)\\ &-\left[\gamma_2^0 + \gamma_2^1\varepsilon_\omega\left(e^{-a_1\tau} - e^{-a_1\tau_0/2}\right) + \gamma_2^2\varepsilon_g\left(e^{-a_2\tau} - e^{-a_2\tau_0/2}\right)\right]\left(F_{S0}^- + \varepsilon_\omega F_{S1}^- + \varepsilon_g F_{S2}^-\right)\\ &-\left[\widehat{\omega}\gamma_3^0 + \gamma_3^0\varepsilon_\omega\left(e^{-a_1\tau} - e^{-a_1\tau_0/2}\right) + \widehat{\omega}\gamma_3^2\varepsilon_g\left(e^{-a_2\tau} - e^{-a_2\tau_0/2}\right)\right]F_0 e^{-\frac{\tau}{\mu_0}}\end{aligned} \tag{8a}$$

$$\begin{aligned}\frac{dF_S^-}{d\tau} = &\left[\gamma_2^0 + \gamma_2^1\varepsilon_\omega\left(e^{-a_1\tau} - e^{-a_1\tau_0/2}\right) + \gamma_2^2\varepsilon_g\left(e^{-a_2\tau} - e^{-a_2\tau_0/2}\right)\right]\left(F_{S0}^+ + \varepsilon_\omega F_{S1}^+ + \varepsilon_g F_{S2}^+\right)\\ &-\left[\gamma_1^0 + \gamma_1^1\varepsilon_\omega\left(e^{-a_1\tau} - e^{-a_1\tau_0/2}\right) + \gamma_1^2\varepsilon_g\left(e^{-a_2\tau} - e^{-a_2\tau_0/2}\right)\right]\left(F_{S0}^- + \varepsilon_\omega F_{S1}^- + \varepsilon_g F_{S2}^-\right)\\ &+\left[\widehat{\omega}\gamma_4^0 + \gamma_4^0\varepsilon_\omega\left(e^{-a_1\tau} - e^{-a_1\tau_0/2}\right) - \widehat{\omega}\gamma_3^2\varepsilon_g\left(e^{-a_2\tau} - e^{-a_2\tau_0/2}\right)\right]F_0 e^{-\frac{\tau}{\mu_0}}\end{aligned} \tag{8b}$$

where $\gamma_4^0 = 1 - \gamma_3^0$. And, Eq. (8) can be rewritten as separate equations for $F_{S0}^\pm$, $F_{S1}^\pm$, and $F_{S2}^\pm$. We obtain the following equations for the scattered flux $F_{S0}^\pm$:

$$\frac{dF_{S0}^+}{d\tau} = \gamma_1^0 F_{S0}^+ - \gamma_2^0 F_{S0}^- - \gamma_3^0\widehat{\omega}F_0 e^{-\frac{\tau}{\mu_0}} \tag{9a}$$

$$\frac{dF_{S0}^-}{d\tau} = \gamma_2^0 F_{S0}^+ - \gamma_1^0 F_{S0}^- + \gamma_4^0\widehat{\omega}F_0 e^{-\frac{\tau}{\mu_0}} \tag{9b}$$

$$F_{S0}^-(0) = 0, F_{S0}^+(\tau_0) = R_{dif}F_{S0}^-(\tau_0) + R_{dir}\mu_0 F_0 e^{-\frac{\tau_0}{\mu_0}} \tag{9c}$$

Eq. (9) is the standard SRT equation for a homogeneous layer [15] and has the following solution:

$$F_{S0}^+ = K_1 e^{k\tau} + \Gamma K_2 e^{-k\tau} + G_1 e^{-\frac{\tau}{\mu_0}} \tag{10a}$$

$$F_{S0}^- = \Gamma K_1 e^{k\tau} + K_2 e^{-k\tau} + G_2 e^{-\frac{\tau}{\mu_0}} \tag{10b}$$

where $K_1 = \frac{\left(\Gamma - R_{dif}\right)\Gamma G_2 e^{-k\tau_0} - \left(G_1 - R_{dir}G_2 - R_{dir}\mu_0 F_0\right)e^{-\frac{\tau_0}{\mu_0}}}{\left(1 - R_{dif}\Gamma\right)e^{k\tau_0} - \left(\Gamma - R_{dif}\right)\Gamma e^{-k\tau_0}}$, $K_2 = -\Gamma K_1 - G_2$, $G_1 = \left[\gamma_3^0\left(\frac{1}{\mu_0} - \gamma_1^0\right) - \gamma_2^0\gamma_4^0\right]\frac{{\mu_0}^2\widehat{\omega}F_0}{1-{\mu_0}^2k^2}$, $G_2 = -\left[\gamma_4^0\left(\frac{1}{\mu_0} + \gamma_1^0\right) + \gamma_2^0\gamma_3^0\right]\frac{{\mu_0}^2\widehat{\omega}F_0}{1-{\mu_0}^2k^2}$, $\Gamma = 1 - \frac{2k}{\gamma_1^0+\gamma_2^0+k}$, and $k^2 = \left(\gamma_1^0 + \gamma_2^0\right)\left(\gamma_1^0 - \gamma_2^0\right)$. And, the equations for the perturbation terms $F_{Si}^\pm$ (i = 1, 2) are

$$\frac{dF_{Si}^{+}}{d\tau} = \gamma_1^0 F_{Si}^{+} - \gamma_2^0 F_{Si}^{-} + \left(e^{-a_i\tau} - e^{-a_i\tau_0/2}\right)\left(\gamma_1^i F_{S0}^{+} - \gamma_2^i F_{S0}^{-}\right) - \gamma_3^{i-1} F_0\left(e^{-a_i\tau} - e^{-a_i\tau_0/2}\right)e^{-\frac{\tau}{\mu_0}} \tag{11a}$$

$$\frac{dF_{Si}^{-}}{d\tau} = \gamma_2^0 F_{Si}^{+} - \gamma_1^0 F_{Si}^{-} + \left(e^{-a_i\tau} - e^{-a_i\tau_0/2}\right)\left(\gamma_2^i F_{S0}^{+} - \gamma_1^i F_{S0}^{-}\right) - \gamma_4^{i-1} F_0\left(e^{-a_i\tau} - e^{-a_i\tau_0/2}\right)e^{-\frac{\tau}{\mu_0}} \tag{11b}$$

$$F_{Si}^{-}(0) = 0, F_{Si}^{+}(\tau_0) = R_{dif} F_{Si}^{-}(\tau_0) \tag{11c}$$

where $\gamma_3^1 = -\gamma_4^1 = \widehat{\omega}\gamma_3^2$. Letting $M_i = F_{Si}^{+} + F_{Si}^{-}$ and $N_i = F_{Si}^{+} - F_{Si}^{-}$, Eq. (11a) and (11b) yields

$$\begin{aligned}\frac{dM_i}{d\tau} = {} & \left(\gamma_1^0 + \gamma_2^0\right)N_i + \left(\psi_i^{+} + \psi_i^{-}\right)e^{-(k+a_i)\tau} + \left(\zeta_i^{+} + \zeta_i^{-}\right)e^{(k-a_i)\tau} + \left(\chi_i^{+} + \chi_i^{-}\right)e^{-\left(a_i+\frac{1}{\mu_0}\right)\tau} \\ & -e^{-a_i\tau_0/2}\left[\left(\psi_i^{+} + \psi_i^{-}\right)e^{-k\tau} + \left(\zeta_i^{+} + \zeta_i^{-}\right)e^{k\tau} + \left(\chi_i^{+} + \chi_i^{-}\right)e^{-\frac{\tau}{\mu_0}}\right]\end{aligned} \tag{12a}$$

$$\begin{aligned}\frac{dN_i}{d\tau} = {} & \left(\gamma_1^0 - \gamma_2^0\right)M_i + \left(\psi_i^{+} - \psi_i^{-}\right)e^{-(k+a_i)\tau} + \left(\zeta_i^{+} - \zeta_i^{-}\right)e^{(k-a_i)\tau} + \left(\chi_i^{+} - \chi_i^{-}\right)e^{-\left(a_i+\frac{1}{\mu_0}\right)\tau} \\ & -e^{-a_i\tau_0/2}\left[\left(\psi_i^{+} - \psi_i^{-}\right)e^{-k\tau} + \left(\zeta_i^{+} - \zeta_i^{-}\right)e^{k\tau} + \left(\chi_i^{+} - \chi_i^{-}\right)e^{-\frac{\tau}{\mu_0}}\right]\end{aligned} \tag{12b}$$

where $\Psi_i^{+} = K_2\left(\gamma_1^i\Gamma - \gamma_2^i\right)$, $\Psi_i^{-} = K_2\left(\gamma_2^i\Gamma - \gamma_1^i\right)$, $\zeta_i^{+} = K_1\left(\gamma_1^i - \gamma_2^i\Gamma\right)$, $\zeta_i^{-} = K_1\left(\gamma_2^i - \gamma_1^i\Gamma\right)$, $\chi_i^{+} = \gamma_1^i G_1 - \gamma_2^i G_2 - \gamma_3^{i-1}F_0$, and $\chi_i^{-} = \gamma_2^i G_1 - \gamma_1^i G_2 + \gamma_4^{i-1}F_0$.

From Eq. (12), we obtain

$$\frac{d^2M_i}{d\tau^2} = k^2 M_i + \eta_{1i}^{+}e^{-(k+a_i)\tau} + \eta_{2i}^{+}e^{(k-a_i)\tau} + \eta_{3i}^{+}e^{-\left(a_i+\frac{1}{\mu_0}\right)\tau} + \eta_{4i}^{+}e^{-k\tau} + \eta_{5i}^{+}e^{k\tau} + \eta_{6i}^{+}e^{-\frac{\tau}{\mu_0}} \tag{13a}$$

$$\frac{d^2N_i}{d\tau^2} = k^2 N_i + \eta_{1i}^{-}e^{-(k+a_i)\tau} + \eta_{2i}^{-}e^{(k-a_i)\tau} + \eta_{3i}^{-}e^{-\left(a_i+\frac{1}{\mu_0}\right)\tau} + \eta_{4i}^{-}e^{-k\tau} + \eta_{5i}^{-}e^{k\tau} + \eta_{6i}^{-}e^{-\frac{\tau}{\mu_0}} \tag{13b}$$

where $\eta_{1i}^{\pm} = \left(\gamma_1^0 \pm \gamma_2^0\right)\left(\psi_i^{+} \mp \psi_i^{-}\right) - (k + a_i)\left(\psi_i^{+} \pm \psi_i^{-}\right)$, $\eta_{2i}^{\pm} = (k - a_i)\left(\zeta_i^{+} \pm \zeta_i^{-}\right) + \left(\gamma_1^0 \pm \gamma_2^0\right)\left(\zeta_i^{+} \mp \zeta_i^{-}\right)$, $\eta_{3i}^{\pm} = \left(\chi_i^{+} \mp \chi_i^{-}\right)\left(\gamma_1^0 \pm \gamma_2^0\right) - \left(a_i + \frac{1}{\mu_0}\right)\left(\chi_i^{+} \mp \chi_i^{-}\right)$, $\eta_{4i}^{\pm} = -e^{-a_i\tau_0/2}\left[\left(\gamma_1^0 \pm \gamma_2^0\right)\left(\psi_i^{+} \mp \psi_i^{-}\right) - k\left(\psi_i^{+} \pm \psi_i^{-}\right)\right]$, $\eta_{5i}^{\pm} = -e^{-a_i\tau_0/2}\left[k\left(\zeta_i^{+} \pm \zeta_i^{-}\right) + \left(\gamma_1^0 \pm \gamma_2^0\right)\left(\zeta_i^{+} \mp \zeta_i^{-}\right)\right]$, and $\eta_{6i}^{\pm} = -e^{-a_i\tau_0/2}\left[\left(\chi_i^{+} \mp \chi_i^{-}\right)\left(\gamma_1^0 \pm \gamma_2^0\right) - \frac{1}{\mu_0}\left(\chi_i^{+} \mp \chi_i^{-}\right)\right]$.

The solutions of Eq. (13) are

$$M_i = A_i^{+}e^{-k\tau} + B_i^{+}e^{k\tau} + P_i^{+}e^{-(k+a_i)\tau} + Q_i^{+}e^{(k-a_i)\tau} + R_i^{+}e^{-\left(a_i+\frac{1}{\mu_0}\right)\tau} - \frac{\eta_{4i}^{+}}{2k}e^{-k\tau} + \frac{\eta_{5i}^{+}}{2k}e^{k\tau} + \frac{\eta_{6i}^{+}\mu_0^2}{1-\mu_0^2k^2}e^{-\frac{\tau}{\mu_0}} \tag{14a}$$

$$N_i = A_i^{-}e^{-k\tau} + B_i^{-}e^{k\tau} + P_i^{-}e^{-(k+a_i)\tau} + Q_i^{-}e^{(k-a_i)\tau} + R_i^{-}e^{-\left(a_i+\frac{1}{\mu_0}\right)\tau} - \frac{\eta_{4i}^{-}}{2k}e^{-k\tau} + \frac{\eta_{5i}^{-}}{2k}e^{k\tau} + \frac{\eta_{6i}^{-}\mu_0^2}{1-\mu_0^2k^2}e^{-\frac{\tau}{\mu_0}} \tag{14b}$$

where $P_i^{\pm} = \frac{\eta_{1i}^{\pm}}{(k+a_i)^2-k^2}$, $Q_i^{\pm} = \frac{\eta_{2i}^{\pm}}{(k-a_i)^2-k^2}$, and $R_i^{\pm} = \frac{\eta_{3i}^{\pm}}{\left(a_i+\frac{1}{\mu_0}\right)^2-k^2} e^{-\frac{\tau}{\mu_0}}$. Finally, we can obtain F_{Si}^- and F_{Si}^+ as

$$F_{Si}^+ = D_{1i}^+ e^{-k\tau} + D_{2i}^+ e^{k\tau} + \varphi_{1i}^+ e^{-(k+a_i)\tau} + \varphi_{2i}^+ e^{(k-a_i)\tau} + \varphi_{3i}^+ e^{-\left(a_i+\frac{1}{\mu_0}\right)\tau} + \varphi_{4i}^+ \tau e^{-k_1\tau} + \varphi_{5i}^+ \tau e^{k\tau} + \varphi_{6i}^+ e^{-\frac{\tau}{\mu_0}} \tag{15a}$$

$$F_{Si}^- = D_{1i}^- e^{-k\tau} + D_{2i}^- e^{k\tau} + \varphi_{1i}^- e^{-(k+a_i)\tau} + \varphi_{2i}^- e^{(k-a_i)\tau} + \varphi_{3i}^- e^{-\left(a_i+\frac{1}{\mu_0}\right)\tau} + \varphi_{4i}^- \tau e^{-k_1\tau} + \varphi_{5i}^- \tau e^{k\tau} + \varphi_{6i}^- e^{-\frac{\tau}{\mu_0}} \tag{15b}$$

where $D_{1i}^{\pm} = A_i^+ \alpha^{\mp} \pm X_i$, $D_{2i}^{\pm} = B_i^+ \alpha^{\pm} \pm Y$, $\alpha^{\pm} = \frac{1}{2}\left(1 \pm \frac{k}{\gamma_1^0+\gamma_2^0}\right)$, $X_i = \frac{e^{-a_i\tau_0/2}\left(\psi_i^+ + \psi_i^-\right)}{2\left(\gamma_1^0+\gamma_2^0\right)} - \frac{\eta_{4i}^+}{4k\left(\gamma_1^0+\gamma_2^0\right)}$,

$Y_i = \frac{e^{-a_i\tau_0/2}\left(\zeta_i^+ + \zeta_i^-\right)}{2\left(\gamma_1^0+\gamma_2^0\right)} + \frac{\eta_{5i}^+}{4k\left(\gamma_1^0+\gamma_2^0\right)}$, $\quad \phi_{1i}^{\pm} = \frac{1}{2}\left(P_i^+ \pm P_i^-\right)$, $\quad \phi_{2i}^{\pm} = \frac{1}{2}\left(Q_i^+ \pm Q_i^-\right)$, $\quad \phi_{3i}^{\pm} = \frac{1}{2}\left(R_i^+ \pm R_i^-\right)$, $\phi_{4i}^{\pm} = -\frac{\eta_{4i}^+ \pm \eta_{4i}^-}{4k}$, $\phi_{5i}^{\pm} = \frac{\eta_{5i}^+ \pm \eta_{5i}^-}{4k}$, and $\phi_{6i}^{\pm} = \frac{\left(\eta_{6i}^+ \pm \eta_{6i}^-\right)\mu_0^2}{1-\mu_0^2k^2}$. B_i and A_i are determined by the boundary conditions as

$$\begin{aligned} B_i^+ &= -\frac{\phi_{1i}^- + \phi_{2i}^- + \phi_{3i}^- + \phi_{6i}^-)\left(\alpha^- - R_{dif}\alpha^+\right)e^{-k\tau_0} + \alpha^+\left[\left(\phi_{1i}^+ - R_{dif}\phi_{1i}^-\right)e^{-(k+a_i)\tau_0} + \left(\phi_{2i}^+ - R_{dif}\phi_{2i}^-\right)e^{(k-a_i)\tau_0}\right]}{\alpha^-\left(\alpha^- - R_{dif}\alpha^+\right)e^{-k\tau_0} - \alpha^+\left(\alpha^+ - R_{dif}\alpha^-\right)e^{k\tau_0}} \\ &+ \frac{\alpha^+\left[\phi_{3i}^+ - R_{dif}\phi_{3i}^-\right)e^{-\left(a_i+\frac{1}{\mu_0}\right)\tau_0} + \phi_{4i}^+ - R_{dif}\phi_{4i}^-)\tau_0 e^{-k\tau_0} + \left(\phi_{5i}^+ - R_{dif}\phi_{5i}^-\right)\tau_0 e^{k\tau_0} + \left(\phi_{6i}^+ - R_{dif}\phi_{6i}^-\right)e^{-\frac{\tau_0}{\mu_0}}\right]}{\alpha^-\left(\alpha^- - R_{dif}\alpha^+\right)e^{-k\tau_0} - \alpha^+\left(\alpha^+ - R_{dif}\alpha^-\right)e^{k\tau_0}} \\ &+ \frac{(X_i + Y_i)\left(\alpha^- - R_{dif}\alpha^+\right)e^{-k\tau_0} + \left(X_i + R_{dif}X_i\right)\alpha^+ e^{-k\tau_0} + \left(Y_i + R_{dif}Y_i\right)\alpha^+ e^{k\tau_0}}{\alpha^-\left(\alpha^- - R_{dif}\alpha^+\right)e^{-k\tau_0} - \alpha^+\left(\alpha^+ - R_{dif}\alpha^-\right)e^{k\tau_0}} \end{aligned} \tag{16a}$$

$$A_i^+ = \frac{1}{\alpha^+}\left(X_i + Y_i - B_i\alpha^- - \phi_{1i}^- - \phi_{2i}^- - \phi_{3i}^- - \phi_{6i}^-\right) \tag{16b}$$

All detailed calculation about solar radiation can be found at [16].

2.2. IRT solution

The azimuthally averaged infrared radiative transfer equation for intensity $I_I(\tau,\mu)$ is [1–4, 10–12]

$$\mu\frac{dI_I(\tau,\mu)}{d\tau} = I_I(\tau,\mu) - \frac{\omega(\tau)}{2}\int_{-1}^{1} I_I(\tau,\mu)P\left(\tau,\mu,\mu'\right)d\mu' - [1-\omega(\tau)]B(T) \tag{17}$$

where μ, τ, $P\left(\tau,\mu,\mu'\right)$, and $\omega(\tau)$ are same as in Eq. (1). $B(T)$ is the Planck function at temperature T, which represents the internal infrared emission of the medium.

The Planck function is approximated lineally as a function of optical depth [2] as

$$B[T(\tau)] = B_0 + \beta\tau \tag{18}$$

where $\beta = (B_1 - B_0)/\tau_0$ and τ_0 are the total optical depth of the medium. The Planck functions B_0 and B_1 are evaluated by using the temperature of the top ($\tau = 0$) and the bottom ($\tau = \tau_0$) of the medium.

According to the two-stream approximation, the intensities can be written as $I_{\mathrm{I}}(\tau, \mu_1) = I_{\mathrm{I}}^{+}(\tau)$ and $I_{\mathrm{I}}(\tau, \mu_{-1}) = I_{\mathrm{I}}^{-}(\tau)$, respectively, where $\mu_1 = -\mu_{-1} = 1/1.66$ is a diffuse factor that converts radiative intensity to flux [17]. $\int_{-1}^{1} I_I(\tau, \mu)P(\tau, \mu, \mu')d\mu'$ can be written as

$$\int_{-1}^{1} I_I(\tau, \mu)P(\tau, \mu, \mu')d\mu' = \left[1 + 3g(\tau)\mu\mu_1\right]I_I^{+}(\tau) + \left[1 + 3g(\tau)\mu\mu_{-1}\right]I_I^{-}(\tau) \tag{19}$$

where $g(\tau)$ is the asymmetry factor.

Using Eqs. (17) and (19), we can obtain

$$\frac{dI_{\mathrm{I}}^{+}(\tau)}{d\tau} = \gamma_1(\tau)I_{\mathrm{I}}^{+}(\tau) - \gamma_2(\tau)I_{\mathrm{I}}^{-}(\tau) - \gamma_3(\tau)B(\tau) \tag{20a}$$

$$\frac{dI_{\mathrm{I}}^{+}(\tau)}{d\tau} = \gamma_2(\tau)I_{\mathrm{I}}^{+}(\tau) - \gamma_1(\tau)I_{\mathrm{I}}^{-}(\tau) + \gamma_3(\tau)B(\tau) \tag{20b}$$

where $\gamma_1(\tau) = \frac{1\text{-}\omega(\tau)(1+g(\tau))/2}{\mu_1}$, $\gamma_2(\tau) = \frac{\omega(\tau)[1-g(\tau)]}{2\mu_1}$, and $\gamma_3(\tau) = \frac{1-\omega(\tau)}{\mu_1}$.

For IRT, we also use Eq. (3) to represent an inhomogeneous medium such as cloud or snow, in which $\omega(\tau)$ and $g(\tau)$ vary with τ. By substituting Eq. (3) into $\gamma_1(\tau)$, $\gamma_2(\tau)$, and $\gamma_3(\tau)$ and by ignoring the second order of the small parameters of ε_ω^2, ε_g^2, and $\varepsilon_\omega\varepsilon_g$, we can obtain

$$\gamma_1(\tau) = \gamma_1^0 + \gamma_1^1\varepsilon_\omega\left(e^{-a_1\tau} - e^{-a_1\tau_0/2}\right) + \gamma_1^2\varepsilon_g\left(e^{-a_2\tau} - e^{-a_2\tau_0/2}\right) \tag{21a}$$

$$\gamma_2(\tau) = \gamma_2^0 + \gamma_2^1\varepsilon_\omega\left(e^{-a_1\tau} - e^{-a_1\tau_0/2}\right) + \gamma_2^2\varepsilon_g\left(e^{-a_2\tau} - e^{-a_2\tau_0/2}\right) \tag{21b}$$

$$\gamma_3(\tau) = \gamma_3^0 + \gamma_3^1\varepsilon_\omega\left(e^{-a_1\tau} - e^{-a_1\tau_0/2}\right) \tag{21c}$$

In the above formula, γ_i^0, γ_i^1, and γ_i^2 (i = 1, 2, 3) are the known factors of $\widehat{\omega}$ and $\widehat{g}$. These known factors are introduced for simplifying original expressions, in which $\gamma_1^0 = \frac{1-\widehat{\omega}\left(1+\widehat{g}\right)/2}{\mu_1}$, $\gamma_2^0 = \frac{\widehat{\omega}\left(1-\widehat{g}\right)}{2\mu_1}$, $\gamma_3^0 = \frac{1-\widehat{\omega}}{\mu_1}$, $\gamma_1^1 = -\frac{1+\widehat{g}}{2\mu_1}$, $\gamma_2^1 = \frac{1-\widehat{g}}{2\mu_1}$, $\gamma_3^1 = -\frac{1}{\mu_1}$, $\gamma_1^2 = \gamma_2^2 = -\frac{\widehat{\omega}}{2\mu_1}$, and $\gamma_3^2 = 0$.

Same as in Eq. (7), the upward and downward intensity can be written as

$$I_{\mathrm{I}}^{+} = I_{\mathrm{I}0}^{+} + \varepsilon_\omega I_{\mathrm{I}1}^{+} + \varepsilon_g I_{\mathrm{I}1}^{+} \tag{22a}$$

$$I_{\mathrm{I}}^{-} = I_{\mathrm{I}0}^{-} + \varepsilon_\omega I_{\mathrm{I}1}^{-} + \varepsilon_g I_{\mathrm{I}1}^{-} \tag{22b}$$

By substituting Eqs. (21)–(22) into Eq. (20), we obtain

$$\begin{aligned}\frac{dI_{\mathrm{I}}^{+}}{d\tau}=&\left[\gamma_1^0+\gamma_1^1\varepsilon_\omega\left(e^{-a_1\tau}-e^{-a_1\tau_0/2}\right)+\gamma_1^2\varepsilon_g\left(e^{-a_2\tau}-e^{-a_2\tau_0/2}\right)\right]\left(I_{\mathrm{I}0}^{+}+\varepsilon_\omega I_{\mathrm{I}1}^{+}+\varepsilon_g I_{\mathrm{I}2}^{+}\right)\\&-\left[\gamma_2^0+\gamma_2^1\varepsilon_\omega\left(e^{-a_1\tau}-e^{-a_1\tau_0/2}\right)+\gamma_2^2\varepsilon_g\left(e^{-a_2\tau}-e^{-a_2\tau_0/2}\right)\right]\left(I_{\mathrm{I}0}^{-}+\varepsilon_\omega I_{\mathrm{I}1}^{-}+\varepsilon_g I_{\mathrm{I}2}^{-}\right)\\&-\left[\gamma_3^0+\gamma_3^1\varepsilon_\omega\left(e^{-a_1\tau}-e^{-a_1\tau_0/2}\right)\right]B(\tau)\end{aligned}\tag{23a}$$

$$\begin{aligned}\frac{dI_{\mathrm{I}}^{-}}{d_\tau}=&\left[\gamma_2^0+\gamma_2^1\varepsilon_\omega\left(e^{-a_1\tau}-e^{-a_1\tau_0/2}\right)+\gamma_2^2\varepsilon_g\left(e^{-a_2\tau}-e^{-a_2\tau_0/2}\right)\right]\left(I_{\mathrm{I}0}^{+}+\varepsilon_\omega I_{\mathrm{I}1}^{+}+\varepsilon_g I_{\mathrm{I}2}^{+}\right)\\&-\left[\gamma_1^0+\gamma_1^1\varepsilon_\omega\left(e^{-a_1\tau}-e^{-a_1\tau_0/2}\right)+\gamma_1^2\varepsilon_g\left(e^{-a_2\tau}-e^{-a_2\tau_0/2}\right)\right]\left(I_{\mathrm{I}0}^{-}+\varepsilon_\omega I_{\mathrm{I}1}^{-}+\varepsilon_g I_{\mathrm{I}2}^{-}\right)\\&+\left[\gamma_3^0+\gamma_3^1\varepsilon_\omega\left(e^{-a_1\tau}-e^{-a_1\tau_0/2}\right)\right]B(\tau)\end{aligned}\tag{23b}$$

By removing the second-order and higher-order perturbation terms, we can also separate Eq. (23) into three equations of $I_{\mathrm{I}i}^{\pm}$ (i = 0, 1, 2). The equations of $I_{\mathrm{I}0}^{\pm}$ can be written as

$$\frac{dI_{\mathrm{I}0}^{+}}{d\tau}=\gamma_1^0 dI_{\mathrm{I}0}^{+}-\gamma_2^0 dI_{\mathrm{I}0}^{-}-\gamma_3^0 B(\tau)\tag{24a}$$

$$\frac{dI_{\mathrm{I}0}^{-}}{d\tau}=\gamma_2^0 I_{\mathrm{I}0}^{+}-\gamma_1^0 I_{\mathrm{I}0}^{-}+\gamma_3^0 B(\tau)\tag{24b}$$

$$I_{\mathrm{I}0}^{-}(0)=0,\ I_{\mathrm{I}0}^{+}(\tau_0)=(1-\varepsilon_s)I_{\mathrm{I}0}^{-}(\tau_0)+\varepsilon_s B(T_s)\tag{24c}$$

where T_s and ε_s are surface temperature and surface emissivity, respectively. Eq. (24) is the standard homogeneous two-stream infrared radiative transfer equation [3, 15] with solutions

$$I_{\mathrm{I}0}^{+}=\alpha^{+}K_0e^{-k(\tau_0-\tau)}+\alpha^{-}H_0e^{-k\tau}+G_1\tau+G_2^{+}\tag{25a}$$

$$I_{\mathrm{I}0}^{-}=\alpha^{-}K_0e^{-k(\tau_0-\tau)}+\alpha^{+}H_0e^{-k\tau}+G_1\tau+G_2^{-}\tag{25b}$$

where $k^2=\left(\gamma_1^0+\gamma_2^0\right)\left(\gamma_1^0-\gamma_2^0\right)$, $\alpha^{\pm}=\frac{1}{2}\left(1\pm\frac{k}{\gamma_1^0+\gamma_2^0}\right)$, $G_1=\frac{\gamma_3^0}{\gamma_1^0-\gamma_2^0}\beta$, $G_2^{\pm}=\frac{\gamma_3^0}{\gamma_1^0-\gamma_2^0}B_0\pm\frac{\beta\gamma_3^0}{k^2}$, $H_0=\frac{\alpha^{-}e^{-k\tau_0}\left[\left(G_2^{+}-RG_2^{-}\right)+(1-R)G_1\tau_0-(1-R)B(T_s)\right]-(\alpha^{+}-R\alpha^{-})G_2^{-}}{\alpha^{+}(\alpha^{+}-R\alpha^{-})-\alpha^{-}\left(\alpha^{-}-R_{dif}\alpha^{+}\right)e^{-2k\tau_0}}$, $K_0=-\frac{\alpha^{+}H_0+G_2^{-}}{\alpha^{-}e^{-k\tau_0}}$, and $R=1-\varepsilon_s$.

The equations for $I_{\mathrm{I}i}^{\pm}$ (i = 1, 2) are

$$\frac{dI_{\mathrm{I}i}^{+}}{d\tau}=\gamma_1^0 I_{\mathrm{I}i}^{+}-\gamma_2^0 I_{\mathrm{I}i}^{-}+\left(e^{-a_i\tau}-e^{-a_i\tau_0/2}\right)\left[\gamma_1^i I_{\mathrm{I}0}^{+}-\gamma_2^i I_{\mathrm{I}0}^{-}-\gamma_3^i B(\tau)\right]\tag{26a}$$

$$\frac{dI_{\mathrm{I}i}^{-}}{d\tau}=\gamma_2^0 I_{\mathrm{I}i}^{+}-\gamma_1^0 I_{\mathrm{I}i}^{-}+\left(e^{-a_i\tau}-e^{-a_i\tau_0/2}\right)\left[\gamma_2^i I_{\mathrm{I}0}^{+}-\gamma_1^i I_{\mathrm{I}0}^{-}+\gamma_3^i B(\tau)\right]\tag{26b}$$

$$I_{\mathrm{I}i}^{-}(0)=0,\ I_{\mathrm{I}i}^{+}(\tau_0)=(1-\varepsilon_s)I_{\mathrm{I}i}^{-}(\tau_0)\tag{26c}$$

Let $M_i=I_{\mathrm{I}i}^{+}+I_{\mathrm{I}i}^{-}$ and $N_i=I_{\mathrm{I}i}^{+}-I_{\mathrm{I}i}^{-}$. Eq. (26a) and (26b) yields

$$\frac{dM_i}{d\tau} = (\gamma_1^0 + \gamma_2^0)N_i + \chi_{1i}^+ e^{-k\tau_0+(k-a_i)\tau} + \chi_{2i}^+ e^{-(k+a_i)\tau} + \chi_{3i}^+ e^{-k(\tau_0-\tau)} + \chi_{4i}^+ e^{-k\tau} + \chi_{5i}^+ + \chi_{6i}^+ e^{-a_i\tau} \quad (27a)$$

$$\frac{dN_i}{d\tau} = (\gamma_1^0 - \gamma_2^0)M_i + \chi_{1i}^- e^{-k\tau_0+(k-a_i)\tau} + \chi_{2i}^- e^{-(k+a_i)\tau} + \chi_{3i}^- e^{-k(\tau_0-\tau)} + \chi_{4i}^- e^{-k\tau} + \chi_{5i}^- + \chi_{6i}^- e^{-a_i\tau} + \chi_{7i}^- \tau + \chi_{8i}^- \tau e^{-a_i\tau} \quad (27b)$$

where $\chi_{1i}^{\pm} = K_0(\alpha^+ \mp \alpha^-)(\gamma_1^i \pm \gamma_2^i)$, $\chi_{2i}^{\pm} = \mp H_0(\alpha^+ \mp \alpha^-)(\gamma_1^i \pm \gamma_2^i)$, $\chi_{3i}^{\pm} = -K_0(\alpha^+ \mp \alpha^-)(\gamma_1^i \pm \gamma_2^i)e^{-a_i\tau_0/2}$, $\chi_{4i}^{\pm} = \pm H_0(\alpha^+ \mp \alpha^-)(\gamma_1^i \pm \gamma_2^i)e^{-a_i\tau_0/2}$, $\chi_{5i}^{+} = -(G_2^+ - G_2^-)(\gamma_1^i + \gamma_2^i)e^{-a_i\tau_0/2}$, $\chi_{5i}^{-} = -(G_2^+ + G_2^-)(\gamma_1^i - \gamma_2^i)e^{-a_i\tau_0/2} + 2B_0\gamma_3^i e^{-a_i\tau_0/2}$, $\chi_{6i}^{+} = (G_2^+ - G_2^-)(\gamma_1^i + \gamma_2^i)$, $\chi_{6i}^{-} = (G_2^+ + G_2^-)(\gamma_1^i - \gamma_2^i) - 2B_0\gamma_3^i$, $\chi_{7i}^{-} = [-2G_1(\gamma_1^i - \gamma_2^i) + 2\beta\gamma_3^i]e^{-a_i\tau_0/2}$, and $\chi_{8i}^{-} = 2G_1(\gamma_1^i - \gamma_2^i) - 2\beta\gamma_3^i$.

From Eq. (27), we can obtain

$$\frac{d^2M_i}{d\tau^2} = k^2M_i + \phi_{1i}^+ e^{-k\tau_0+(k-a_i)\tau} + \phi_{2i}^+ e^{-(k+a_i)\tau} + \phi_{3i}^+ e^{-k(\tau_0-\tau)} + \phi_{4i}^+ e^{-k\tau} + \phi_{5i}^+ + \phi_{6i}^+ e^{-a_i\tau} + \phi_{7i}^+ \tau + \phi_{8i}^+ \tau e^{-a_i\tau} \quad (28a)$$

$$\frac{d^2N_i}{d\tau^2} = k^2N_i + \phi_{1i}^- e^{-k\tau_0+(k-a_i)\tau} + \phi_{2i}^- e^{-(k+a_i)\tau} + \phi_{3i}^- e^{-k(\tau_0-\tau)} + \phi_{4i}^- e^{-k\tau} + \phi_{5i}^- + \phi_{6i}^- e^{-a_i\tau} + \phi_{8i}^- \tau e^{-a_i\tau} \quad (28b)$$

where $\phi_{1i}^{\pm} = (\gamma_1^0 \pm \gamma_2^0)\chi_{1i}^{\mp} + (k - a_i)\chi_{1i}^{\pm}$, $\phi_{2i}^{\pm} = (\gamma_1^0 \pm \gamma_2^0)\chi_{2i}^{\mp} - (k + a_i)\chi_{2i}^{\pm}$, $\phi_{3i}^{\pm} = (\gamma_1^0 \pm \gamma_2^0)\chi_{3i}^{\mp} + k\chi_{3i}^{\pm}$, $\phi_{4i}^{\pm} = (\gamma_1^0 \pm \gamma_2^0)\chi_{4i}^{\mp} - k\chi_{4i}^{\pm}$, $\phi_{5i}^{+} = (\gamma_1^0 + \gamma_2^0)\chi_{5i}^{-}$, $\phi_{5i}^{-} = (\gamma_1^0 - \gamma_2^0)\chi_{5i}^{+} + \chi_{7i}^{-}$, $\phi_{6i}^{+} = (\gamma_1^0 + \gamma_2^0)\chi_{6i}^{-} - a_i\chi_{6i}^{+}$, $\phi_{6i}^{-} = (\gamma_1^0 - \gamma_2^0)\chi_{6i}^{+} - a_i\chi_{6i}^{-} + \chi_{8i}^{-}$, $\phi_{7i}^{+} = (\gamma_1^0 + \gamma_2^0)\chi_{7i}^{-}$, $\phi_{8i}^{+} = (\gamma_1^0 + \gamma_2^0)\chi_{8i}^{-}$, and $\phi_{8i}^{-} = -a_i\chi_{8i}^{-}$. Thus, the solutions are

$$M_i = K_{1i}e^{-k(\tau_0-\tau)} + H_{1i}e^{-k\tau} + P_{1i}^+ e^{-k\tau_0+(k-a_i)\tau} + P_{2i}^+ e^{-(k+a_i)\tau} + P_{3i}^+ \tau e^{-k(\tau_0-\tau)} + P_{4i}^+ \tau e^{-k\tau} + P_{5i}^+ + P_{6i}^+ e^{-a_i\tau} + P_{7i}^+ \tau + P_{8i}^+ \tau e^{-a_i\tau} \quad (29a)$$

$$N_i = K_{2i}e^{-k(\tau_0-\tau)} + H_{2i}e^{-k\tau} + P_{1i}^- e^{-k\tau_0+(k-a_i)\tau} + P_{2i}^- e^{-(k+a_i)\tau} + P_{3i}^- \tau e^{-k(\tau_0-\tau)} + P_{4i}^- \tau e^{-k\tau} + P_{5i}^- + P_{6i}^- e^{-a_i\tau} + P_{8i}^- \tau e^{-a_i\tau} \quad (29b)$$

where $P_{1i}^{\pm} = \frac{\phi_{1i}^{\pm}}{(k-a_i)^2-k^2}$, $P_{2i}^{\pm} = \frac{\phi_{2i}^{\pm}}{(k+a_i)^2-k^2}$, $P_{3i}^{\pm} = \frac{\phi_{3i}^{\pm}}{2k}$, $P_{4i}^{\pm} = -\frac{\phi_{4i}^{\pm}}{2k}$, $P_{5i}^{\pm} = -\frac{\phi_{5i}^{\pm}}{k^2}$, $P_{6i}^{\pm} = \frac{\phi_{6i}^{\pm}(a_i^2-k^2)+2a_i\phi_{8i}^{\pm}}{(a_i^2-k^2)^2}$, $P_{7i}^{+} = -\frac{\phi_{7i}^{+}}{k^2}$, and $P_{8i}^{+} = \frac{\phi_{8i}^{+}}{a_i^2-k^2}$.

The expressions of $I_{1i}^{\pm}$ are

$$I_{1i}^+ = D_{1i}^+ e^{-k(\tau_0-\tau)} + D_{2i}^+ e^{-k\tau} + \sigma_{1i}^+ e^{-k\tau_0+(k-a_i)\tau} + \sigma_{2i}^+ e^{-(k+a_i)\tau} + \sigma_{3i}^+ \tau e^{-k(\tau_0-\tau)} + \sigma_{4i}^+ \tau e^{-k\tau} + \sigma_{5i}^+ + \sigma_{6i}^+ e^{-a_i\tau} + \sigma_{7i}\tau + \sigma_{8i}^+ \tau e^{-a_i\tau} \quad (30a)$$

$$I_{1i}^- = D_{1i}^- e^{-k(\tau_0-\tau)} + D_{2i}^- e^{-k\tau} + \sigma_{1i}^- e^{-k\tau_0+(k-a_i)\tau} + \sigma_{2i}^- e^{-(k+a_i)\tau} + \sigma_{3i}^- \tau e^{-k(\tau_0-\tau)} + \sigma_{4i}^- \tau e^{-k\tau} + \sigma_{5i}^- + \sigma_{6i}^- e^{-a_i\tau} + \sigma_{7i}\tau + \sigma_{8i}^- \tau e^{-a_i\tau} \quad (30b)$$

where $D_{1i}^{\pm} = K_{1i}\alpha^{\pm} \pm X_i$, $D_{2i}^{\pm} = H_{1i}\alpha^{\mp} \pm Y_i$, $X_i = \frac{P_{3i}^{+} - \chi_{3i}^{+}}{2\left(\gamma_1^0 + \gamma_2^0\right)}$, $Y_i = \frac{P_{4i}^{+} - \chi_{4i}^{+}}{2\left(\gamma_1^0 + \gamma_2^0\right)}$, $\sigma_{ji}^{\pm} = \frac{1}{2}\left(P_{ji}^{+} \pm P_{ji}^{-}\right)$. (j = 1, 2, 3, 4, 5, 6, 8), $\sigma_{7i} = \frac{1}{2}P_{7i}^{+}$, and K_{1i} and H_{1i} are determined by boundary conditions. By substituting Eq. (30) into the boundary conditions of Eq. (26c), we can obtain

$$H_{1i} = \frac{(\alpha^{+} - R\alpha^{-})\left(X_i e^{-k\tau_0} + Y_i - \sigma_{1i}^{-}e^{-k\tau_0} - \sigma_{2i}^{-} - \sigma_{5i}^{-} - \sigma_{6i}^{-}\right) + \alpha^{-}e^{-k\tau_0}\left[(R+1)X_i + (R+1)Y_i e^{-k\tau_0}\right]}{\alpha^{+}\left(\alpha^{+} - R_{dif}\alpha^{-}\right) - \alpha^{-}\left(\alpha^{-} - R_{dif}\alpha^{-}\right)e^{-2k\tau_0}}$$
$$- \frac{\alpha^{-}e^{-k\tau_0}\left[\left(R\sigma_{1i}^{-} - \sigma_{1i}^{+}\right)e^{-a_i\tau_0} + \left(R\sigma_{2i}^{-} - \sigma_{2i}^{+}\right)e^{-(k+a_i)\tau_0} + \left(R\sigma_{3i}^{-} - \sigma_{3i}^{+}\right)\tau_0 + \left(R\sigma_{4i}^{-} - \sigma_{4i}^{+}\right)\tau_0 e^{-k\tau_0}\right]}{\alpha^{+}\left(\alpha^{+} - R_{dif}\alpha^{-}\right) - \alpha^{-}\left(\alpha^{-} - R_{dif}\alpha^{-}\right)e^{-2k\tau_0}}$$
$$- \frac{\alpha^{-}e^{-k\tau_0}\left[\left(R\sigma_{5i}^{-} - \sigma_{5i}^{+}\right) + \left(R\sigma_{6i}^{-} - \sigma_{6i}^{+}\right)e^{-a_i\tau_0} + (R-1)\sigma_{7i}\tau_0 + \left(R\sigma_{8i}^{-} - \sigma_{8i}^{+}\right)\tau_0 e^{-a_i\tau_0}\right]}{\alpha^{+}\left(\alpha^{+} - R_{dif}\alpha^{-}\right) - \alpha^{-}\left(\alpha^{-} - R_{dif}\alpha^{-}\right)e^{-2k\tau_0}} \tag{31a}$$

$$K_{1i} = \frac{1}{\alpha^{-}e^{-k\tau_0}}\left(X_i e^{-k\tau_0} + Y_i - \alpha^{+}H_{1i} - \sigma_{1i}^{-}e^{-k\tau_0} - \sigma_{2i}^{-} - \sigma_{5i}^{-} - \sigma_{6i}^{-}\right) \tag{31b}$$

Finally, the upward and downward fluxes are obtained by

$$F_{\mathrm{I}}^{+}(0) = \pi I_{\mathrm{I}}^{+}(0) \tag{32a}$$

$$F_{\mathrm{I}}^{-}(\tau_0) = \pi I_{\mathrm{I}}^{-}(\tau_0) \tag{32b}$$

All detailed calculation about solar radiation can be found at [18].

3. Results and discussion

We apply the two schemes to idealized medium to investigate its accuracy, and the result has been shown on [16] and [18].

For true cloud medium, because ice clouds' optical properties strongly depend on the complex particle habits [19–21]. Therefore, we limit our discussion here to water cloud only. According to the observation, the internal LWC (g m^{-3}) and droplet radius of the cloud tend to increase with height [22]. To take this feature into account, LWC and droplet cross-sectional area (DCA; cm^{-2}, m^{-3}) should increase linearly from the cloud base to the position near the top of the cloud:

$$\mathrm{LWC} = 0.22 + 0.00008z \tag{33a}$$

$$\mathrm{DCA} = 100 + z \tag{33b}$$

where $0 < z < z_0$. The terms z and z_0 denote the height from the cloud base and the height of the cloud top, respectively. From Eq. (33a) to (33b), the cloud effective radius (r_e; μm) and liquid water path (LWP; g m^{-2}) can be obtained:

$$r_e(z) = \frac{3}{4\rho}\frac{\mathrm{LWC}}{\mathrm{DCA}}10^{10} \tag{34a}$$

$$\mathrm{LWP} = \int_0^{z_0} \mathrm{LWC}\,dz \tag{34b}$$

http://dx.doi.org/10.5772/intechopen.77147

where ρ (g m^{-3}) is the liquid water density. In this case, LWC varies from 0.22 to 0.30 g m^{-3}, and r_e varies from 2.06 to 16.50 μm, in which both ranges are consistent with observation [23]. According to [24], we choose LWP = 260 (g m^{-2}) to represent low cloud. In the benchmark calculations, z_0 is divided into 100 internal homogeneous sub-layers, although other numbers can be chosen (e.g., 200). In principle, more internal sub-layers should result in more accurate results. We use 100 internal sub-layers throughout this study because having any more makes little difference to the calculated results. Using 100 sub-layers are sufficiently accurate to resolve the vertical internal inhomogeneity of the medium. We use the optical properties of a

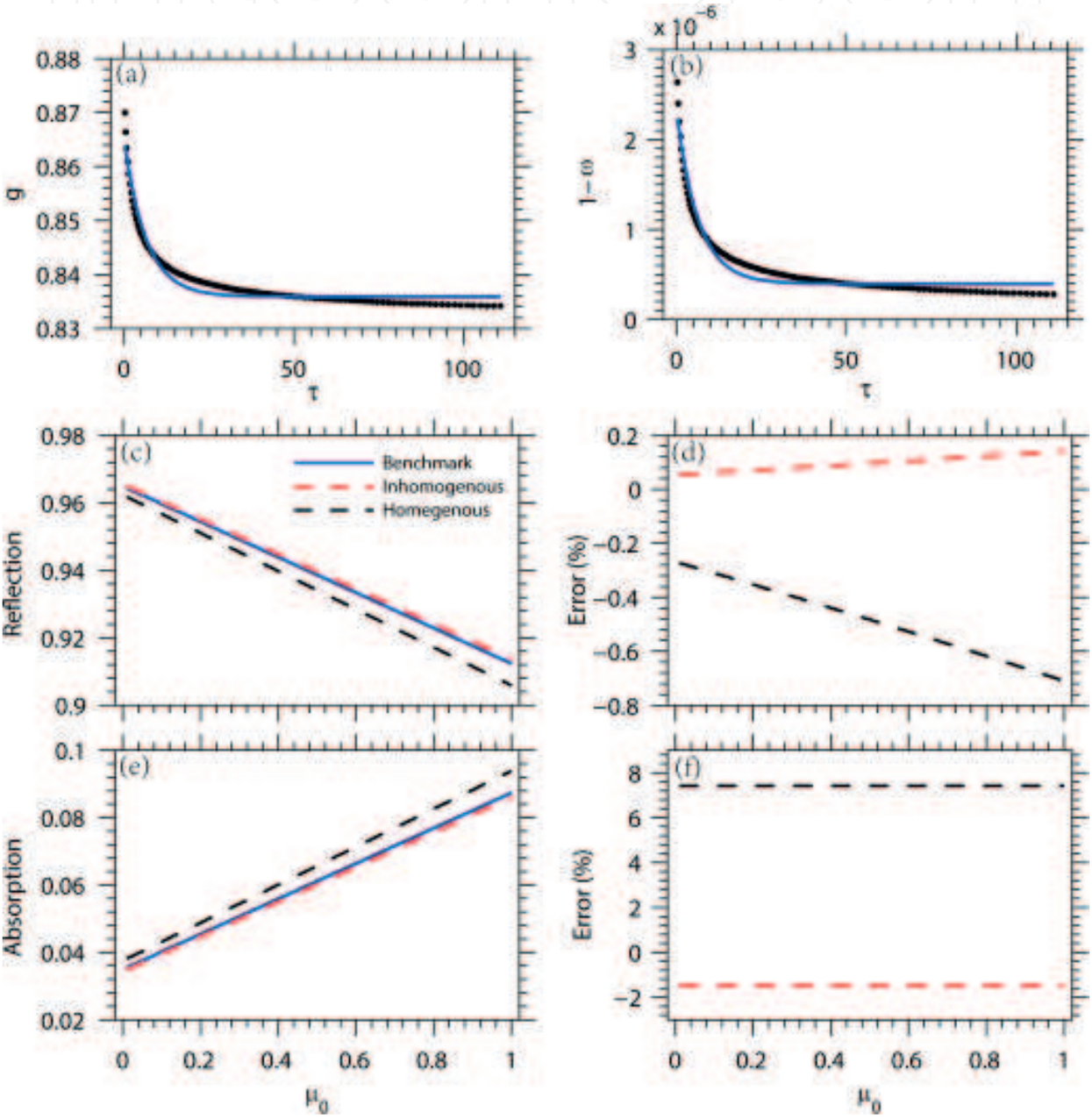

Figure 1. For the band of 0.25–0.69 μm, (a-b) show cloud asymmetry factor/single-scattering albedo versus cloud optical depth (a for asymmetry factor; b for single-scattering albedo), (c-d) show the reflectance/absorptance versus solar zenith angle (c for reflectance; d for absorptance) and (e-f) show the relative errors of the homogeneous and inhomogeneous solutions (e for reflectance error, f for absorptance error).

water cloud in the solar spectral band of 0.25–0.69 μm and at 0.94 μm and in the infrared spectral band of 5–8 μm and 11 μm.

In **Figure 1a** and **b**, the benchmark values of the inhomogeneous IOPs and the parameterized results for the spectral band of 0.25–0.69 μm are shown. The parameterized inhomogeneous IOPs are

$$1-\omega(\tau)=3.979\times10^{-7}-1.897\times10^{-6}\left(e^{-0.1539\tau}-e^{-0.1539\tau_0/2}\right) \tag{35a}$$

$$g(\tau)=0.8359+0.0289\left(e^{-0.1539\tau}-e^{-0.1539\tau_0/2}\right) \tag{35b}$$

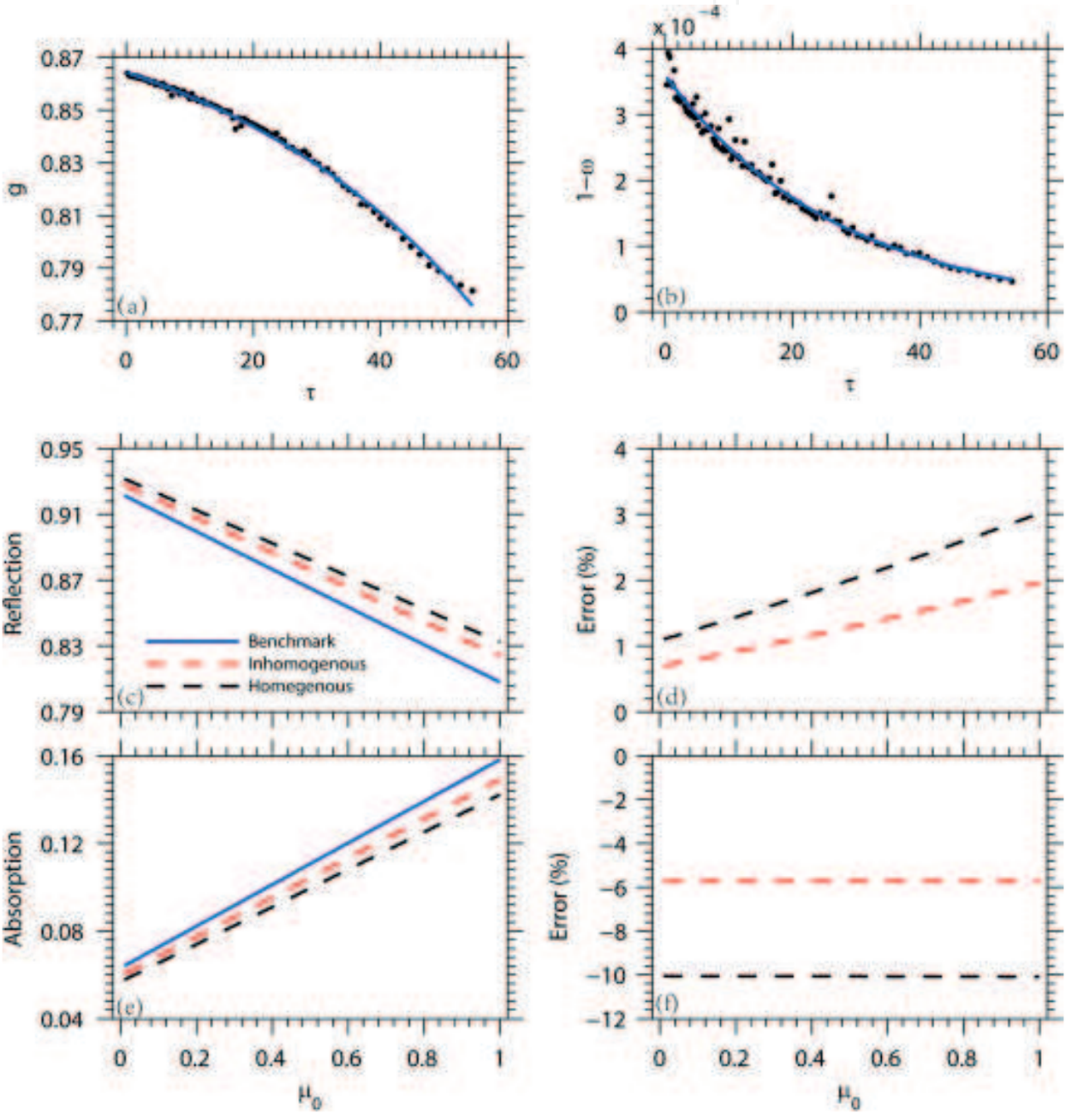

Figure 2. Same as **Figure 1** but for the wavelength 0.94 μm.

where $\tau_0 = 110.84$. The corresponding results for reflection and absorption are shown in **Figure 1c–f**. For reflection, the relative error with the homogeneous solution increases from 0.25 to 0.71% as μ_0 increases from 0.01 to 1, whereas the relative error with the inhomogeneous solution increases from 0.05 to 0.14%. For absorption, the relative error is not sensitive to μ_0; it is around 7.4% with the homogeneous solution but around only 1.4% with the inhomogeneous solution.

In **Figure 2a** and **b**, the benchmark values of the inhomogeneous IOPs and the parameterized results for the wavelength 0.94 μm are shown. The parameterized inhomogeneous IOPs are

$$1 - \omega(\tau) = 1.936 \times 10^{-4} - 5.263 \times 10^{-4}\left(e^{-0.0357\tau} - e^{-0.0357\tau_0/2}\right) \tag{36a}$$

$$g(\tau) = 0.8321 - 0.0403\left(e^{0.0218\tau} - e^{0.0218\tau_0/2}\right) \tag{36b}$$

where $\tau_0 = 54.46$. **Figure 2c–f** shows the corresponding results for reflection and absorption. For reflection, the relative error with the homogeneous solution increases from 1.1 to 3.0% as μ_0 increases from 0.01 to 1, whereas the relative error with the inhomogeneous solution increases from 0.7 to 2.0%. For absorption, the relative error is not sensitive to μ_0; it is around 10% with the homogeneous solution but around only 5.7% with the inhomogeneous solution.

The benchmark values of IOPs and parameterized results for the band of 5–8 μm are shown in **Figure 3a** and **b**. Here, we assume

$$\omega(\tau) = 0.6757 - 0.3697\left(e^{-0.0142\tau} - e^{-0.0142\tau_0/2}\right) \tag{37a}$$

$$g(\tau) = 0.8644 + 0.1023\left(e^{-0.0155\tau} - e^{0.0155\tau_0/2}\right) \tag{37b}$$

where $\tau_0 = 55.85$. For upward emissivity (**Figure 3c** and **d**), the relative errors of both solutions are not sensitive to $F_{\mathrm{I}}^{+}(\tau_0)$; the errors are around -3% for homogeneous solution and around 1% for inhomogeneous solution. For downward emissivity (**Figure 3e** and **f**), the relative error of homogeneous solution is 4% when $F_{\mathrm{I}}^{+}(\tau_0) = 0$, while the error of inhomogeneous solution is only 1%. With $F_{\mathrm{I}}^{+}(\tau_0)$ increasing from 0 to $5\pi B(T)$, the error of homogeneous solution decreases to 0 firstly but then negatively increases to around -10%. The error of inhomogeneous solution shows a similar decreasing-increasing pattern, but the negative increase only reaches about -2%.

The benchmark values of IOPs and parameterized results for the band of 11 μm are shown in **Figure 4a** and **b**. In this case, we assume

$$\omega(\tau) = 0.4623 - 0.2155\left(e^{-0.1018\tau} - e^{-0.1018\tau_0/2}\right) \tag{38a}$$

$$g(\tau) = 0.9118 - 0.0083\left(e^{0.1087\tau} - e^{0.1087\tau_0/2}\right) \tag{38b}$$

where $\tau_0 = 28.23$. For upward emissivity (**Figure 4c** and **d**), the relative error of homogeneous solution is -1.2%, while the error of inhomogeneous solution is less than 0.5%. For downward emissivity (**Figure 4e** and **f**), with $F_{\mathrm{I}}^{+}(\tau_0)$ increasing from 0 to $5\pi B(T)$, the error of homogeneous (inhomogeneous) solution varies from 3 to -11% (from 0 to -1%).

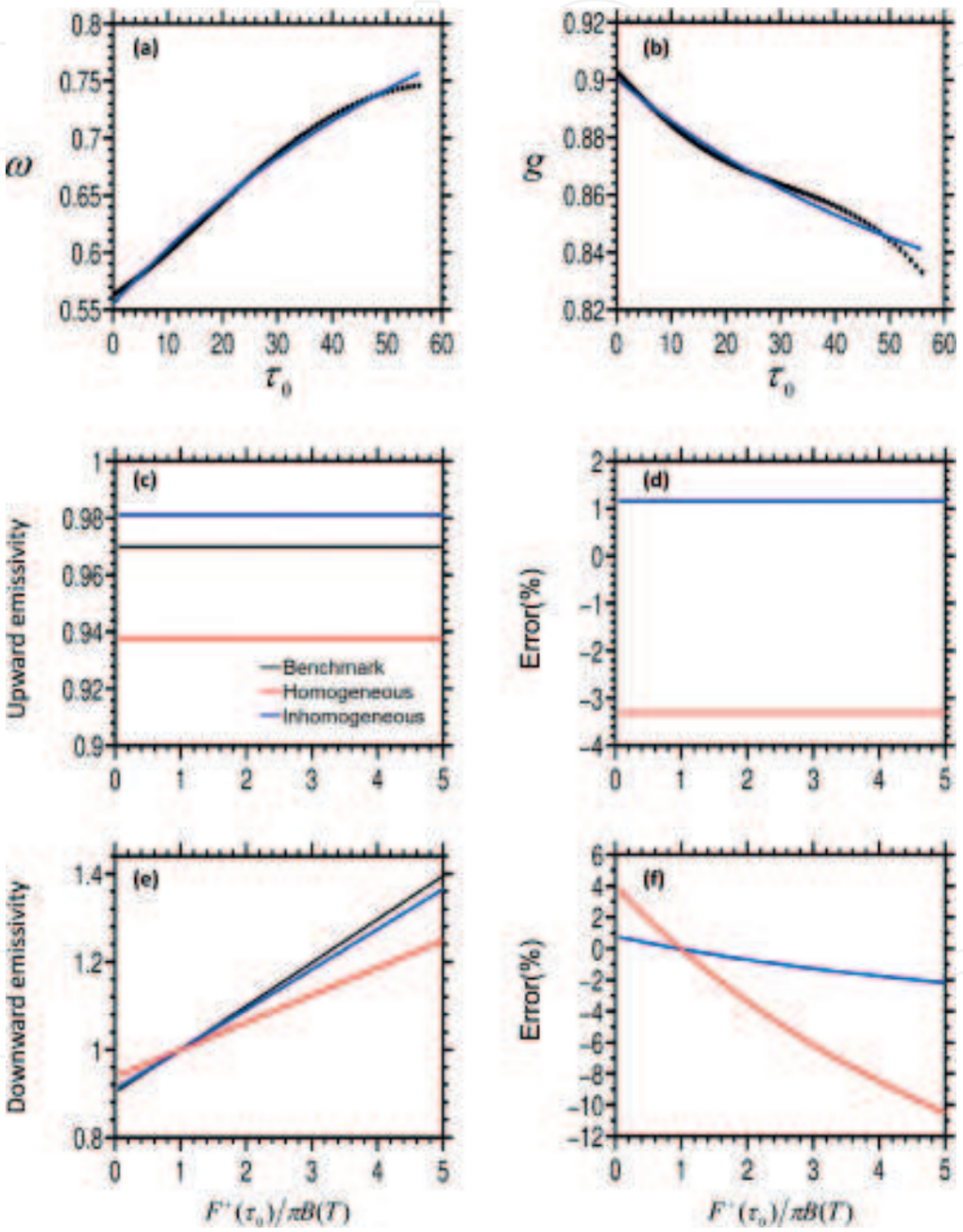

Figure 3. For the band of 5-8 μm, (a-b) show the cloud single-scattering albedo and asymmetry factor versus cloud optical depth, black dots represent the exact values and the blue lines is the fitting results (a for single-scattering albedo; b for asymmetry factor); (c-d) show the upward/downward emissivity versus the ratio of the radiation incident from the bottom to the internal infrared emission of the medium (c for upward emissivity; d for downward emissivity) and (e-f) show the relative errors of the homogeneous and inhomogeneous solutions (e for upward emissivity; f for downward emissivity).

http://dx.doi.org/10.5772/intechopen.77147

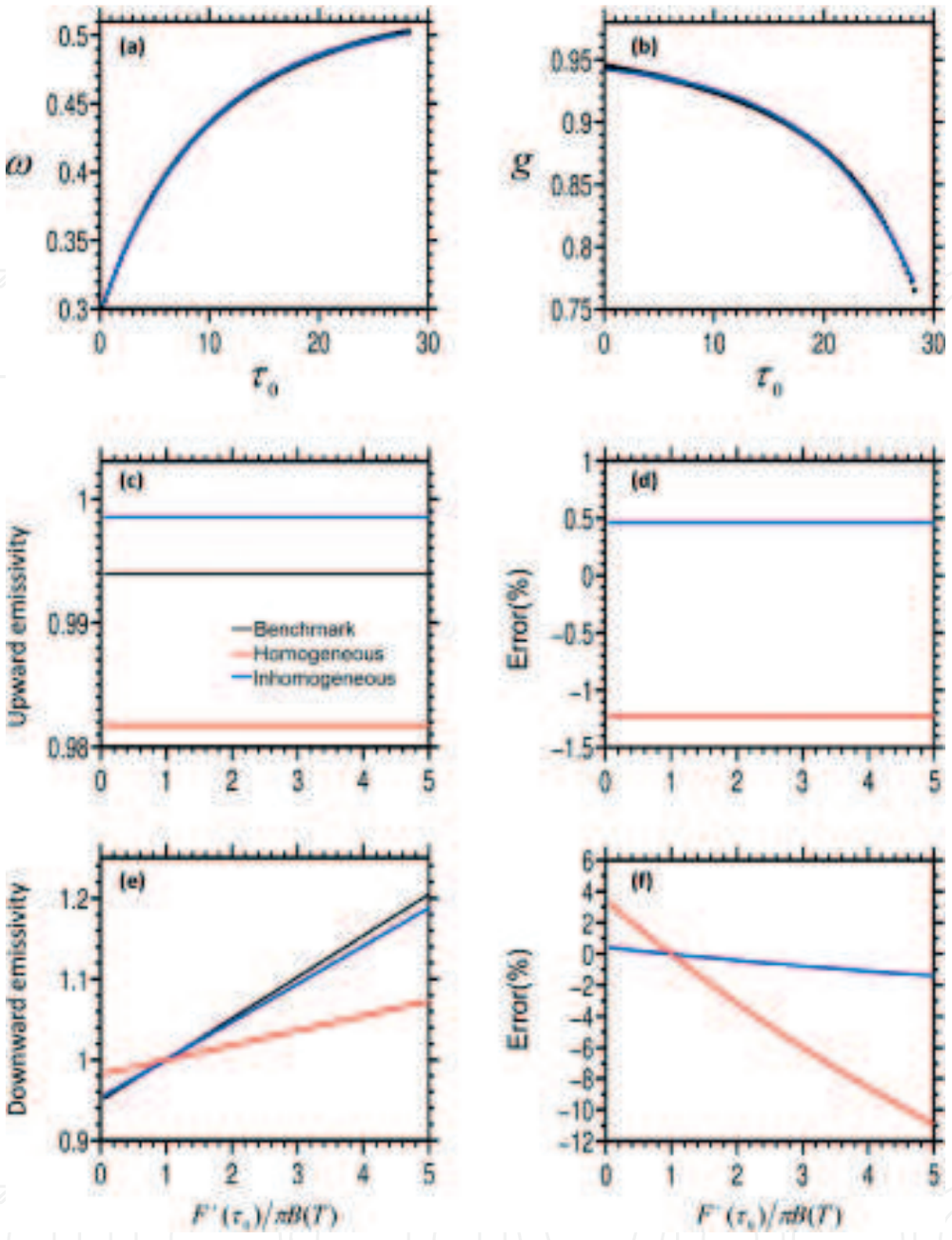

Figure 4. Same as **Figure 3** but for the wavelength of 11 μm.

4. Summary and conclusions

In the above, we have considered the vertically inhomogeneous structures of only cloud and snow, whereas all physical quantities in the atmosphere are vertically inhomogeneous (e.g., the concentrations of all types of gases and aerosols). In current climate models, the vertical layer resolution is far from that required to resolve such vertical inhomogeneity. In this study, we have proposed a new inhomogeneous SRT/IRT solution to address the vertical inhomogeneity

by introducing an internal variation of IOPs inside each model layer. This scheme is based on standard perturbation theory and allows us to use the standard solar Eddington solution and standard infrared two-stream solution for homogeneous layers to identify a zeroth-order equation and a first-order equation that includes the inhomogeneous effect. The new SRT/IRT solution can accurately express the inhomogeneous effect in each model layer, and it reduces to the standard solution when the medium is homogeneous.

The new inhomogeneous SRT/IRT solution is a good way to resolve cloud vertical inhomogeneity. In the spectral band of 0.25–0.69 μm, the relative error in the inhomogeneous SRT solution is no more than 1.4%, whereas the error with the homogeneous SRT solution can be up to 7.4%. At the specific wavelength of 0.94 μm, the relative error with the inhomogeneous solution is not more than 5.7% but can be up to 10% with the homogeneous SRT solution. In the band of 5–8 μm, the homogeneous IRT solution is not sensitive to $F_{\mathrm{I}}^{+}(\tau_0)$, and its relative error may reach −3.2% for upward emissivity, whereas the error of inhomogeneous IRT solution is only 1%. With $F_{\mathrm{I}}^{+}(\tau_0)$ increasing from 0 to $5\pi B(T)$, the error of downward emissivity for homogeneous solution varies from 4 to −10%, while the error ranges from 1 to −2% for inhomogeneous IRT solution. In the band of 11 μm, the relative error of homogeneous IRT solution is around −1.2% for upward emissivity, and the error of inhomogeneous IRT solution is only less than 0.5%. For downward emissivity, the maximum error of homogeneous IRT solution can be up to −11%, and the maximum error of inhomogeneous IRT solution is only around −1% when $F_{\mathrm{I}}^{+}(\tau_0) = 5\pi B(T)$.

In specific spectral bands or at particular wavelengths, the vertical variations in IOPs can typically be fitted easily into Eq. (3) to obtain the required parameters. A simple fitting program can be easily incorporated into a climate model to produce the inhomogeneous IOPs of stratocumulus clouds. If no such cloud inhomogeneity information is available in the current climate models, the vertical variation rates of cloud LWC and DCA can be derived empirically from observations, which show that the vertical variation rates of LWC and DCA in stratocumulus clouds are not very different [5, 7, 8].

In this study, we presented only a single-layer inhomogeneous SRT/IRT solution. To implement the new solution in a climate model, the adding process for layer-to-layer connections has to be solved. Under the homogeneous condition, the single-layer result in reflection and transmission is the same for an upward path and a downward path, but this is not true for an inhomogeneous layer. Therefore, the adding process has to be modified. We will present an algorithm for this multilayer adding process in our next study, in which the climatic impact of inhomogeneous clouds and inhomogeneous snows will be explored. The code base for the inhomogeneous SRT/IRT solution is available from the authors upon request.

Acknowledgements

The work is supported by National Natural Science Foundation of China (41675003) and the Priority Academic Program Development of Jiangsu Higher Education Institutions (PAPD).

Author details

Yi-Ning Shi[1], Feng Zhang[1]*, Jia-Ren Yan[1], Qiu-Run Yu[1] and Jiangnan Li[2]

*Address all correspondence to: fengzhang@nuist.edu.cn

1 Key Laboratory of Meteorological Disaster, Ministry of Education, Nanjing University of Information Science and Technology, Nanjing, China

2 Canadian Centre For Climate Modelling and Analysis, Environment and Climate Change Canada, University of Victoria, Victoria, British Columbia, Canada

References

[1] Lenoble J. Radiative Transfer in Scattering and Absorbing Atmospheres: Standard Computational Procedures. Hampton, VA: A. Deepak Publishing; 1985. 314 pp

[2] Toon OB, McKay CP, Ackerman TP. Rapid calculation of radiative heating rates and photodissociation rates in inhomogeneous multiple scattering atmospheres. Journal of Geophysical Research. 1989;**94**:16287-16301

[3] Fu Q, Liou KN, Cribb MC, Charlock TP, Grossman A. Multiple scattering parameterization in thermal infrared radiative transfer. Journal of the Atmospheric Sciences. 1997;**54**: 2799-2812

[4] Li J, Dobbie S, Raisanen P, Min Q. Accounting for unresolved cloud in solar radiation. Quarterly Journal of the Royal Meteorological Society. 2005;**131**:1607-1629

[5] Vane D, Tourville N, Stephens G, Kanekiewicz A. New observations of hurricanes from the cloudsat radar. In: AGU Fall Meeting Abstracts. 2006:A13A-0885

[6] Boutle IA, Abel SJ, Hill PG, Morcrette CJ. Spatial variability of liquid cloud and rain: Observations and microphysical effects. Quarterly Journal of the Royal Meteorological Society. 2014;**140**:583-594

[7] Young AH, Bates J, Curry J. Application of cloud vertical structure from cloudsat to investigate modis-derived cloud properties of cirriform, anvil and deep convective clouds. Journal of Geophysical Research. 2013;**118**:4689-4699

[8] Luo ZJ, Jeyaratnam J, Iwasaki S, et al. Convective vertical velocity and cloud internal vertical structure: An a-train perspective. Geophysical Research Letters. 2014;**41**:723-729

[9] Chen MN, Lu CS, Liu YG. Variation in entrainment rate and relationship with cloud microphysical properties on the scale of 5m. Scientific Bulletin. 2015;**60**:707-717

[10] Li J, Geldart DJW, Chylek P. Solar radiative transfer in clouds with vertical internal homogeneity. Journal of the Atmospheric Sciences. 1994;**51**:2542-2552

[11] Liou KN. An Introduction to Atmospheric Radiation. 3d ed. USA: Academic Press; 2002. 583 pp

[12] Mackel A, Mitchell DL, Bremen LV. Monte Carlo radiative transfer calculations for inhomogeneous mixed phase clouds. Physics and Chemistry of the Earth, Part B. 1998;**24**:37-241

[13] von Salzen K et al. The Canadian fourth generation atmospheric global climate model (CANAM4). Part I: Representation of physical processes. Atmosphere-Ocean. 2013;**51**: 104-125

[14] Kato T. Perturbation Theory of Linear Operator. Germany: Spring-Verlag; 1966. 18 p

[15] Meador WE, Weaver RE. Two-stream approximation to radiative transfer in planetary atmospheres: A unified description of existing methods and a new improvement. Journal of the Atmospheric Sciences. 1988;**37**:630-643

[16] Zhang F, Jia-Ren Yan J, Li K, Wu H, Iwabuchi, Yi-Ning Shi. A new radiative transfer method for solar radiation in a vertically internally inhomogeneous medium. Journal of the Atmospheric Sciences. 2018;**75**:41-55

[17] Elsasser WM. Heat Transfer by Infrared Radiation in the Atmosphere. USA: Harvard University Press; 1942. 107 p

[18] Shi Yi-Ning F, Zhang, Jia-Ren Yan H, Iwabuchi, Zhen Wang. The standard perturbation method for infrared radiative transfer in a vertically internally inhomogeneous scattering medium. Journal of Quantitative Spectroscopy and Radiative Transfer. 2018;**213**:149-158

[19] Husi L, Nakajiama TY, Matsui TN. Development of an ice crystal scattering database for the global change observation mission/second generation global imager satellite mission: Investigating the refractive index grid system and potential retrieval error. Applied Optics. 2012;**51**:6172-6178

[20] Husi L, Ishimoto H, Jerome R, et al. Investigation of ice particle habits to be used for ice cloud remote sensing for the gcom-c satellite mission. Atmospheric Chemistry and Physics. 2016;**8**:4787-4798

[21] Yang P, Liou K, Bi L, Liu C, Yi B, Baum B. On the radiative properties of ice clouds: Light scattering, remote sensing and radiation parameterization. Advances in Atmospheric Sciences. 2015;**32**

[22] Noonkester VR. Droplet spectra observed in marine stratus cloud layers. Journal of the Atmospheric Sciences. 1984;**41**:829-845

[23] Chen R, Wood R, Li Z, et al. Studying the vertical variation of cloud droplet effective radius using ship and space-borne remote sensing data. Journal of Geophysical Research. 2008;**113**:762-770

[24] Fu Q. Parameterization of radiative processes in vertical nonhomogeneous multiple scattering atmospheres [PhD thesis]. University of Utah; 1991. 259 pp